JOURNAL OF MECHANICAL ENGINEERING AND SCIENCES
ISSN: 2289-4659 e-ISSN: 2231-8380
VOLUME 18, ISSUE 1, 2024, 9872 – 9882
DOI: https://doi.org/10.15282/jmes.18.1.2024.6.0781

RESEARCH ARTICLE

Performance of tri-tubular conical energy absorber under axial compression

A. A. Khalid* and S. M. Rohaizan

Mechanical Engineertng Department, Faculty of Engineering, Universiti Teknologi Brunei, Tungku link, Gadong, BE1410, Brunei Darussalam
Phone: +6738298814, Fax.: +6732461035

ABSTRACT - Quasi static axial compression loading on tri-tubular cone (TC) has been carried out using LS-DYNA finite element analysis method. Tri-tubular cones of three arrangements; the first arrangement (model TC-1) consists of cone heights of 50 mm, 75 mm and 100 mm where the inner cone is the maximum height. The second arrangement (model TC-2) consists of cone heights of 100 mm, 75 mm, and 50 mm where the outer cone is the maximum height. The third arrangement (model TC-3) consists of three cones of the same height of 100 mm. Cone semi vertex angle of 20^{o} was maintained for all tri-tubular cones tested. Materials used for this research are glass, jute and jute-glass/epoxy. Crashworthiness analyses were performed to investigate the effect of material used, and tri-tubular cone arrangement on peak load. Crush efficiency, and absorbed energy were drawn and discussed. Failure mechanism of the fractured specimens was also discussed. Effect of number of layers and fiber stacking sequence were also investigated. Results show that the cone arrangement TC-3 gives better performance than the cone arrangement TC-2 followed by the cone arrangement TC-1. Maximum load obtained by tri-tubular cone type TC-3 was found higher 7.09% and 14.96% than TC-2 and TC-1 respectively for glass/epoxy. Material saving was achieved by using tri-tubular cones of different heights under compression. Material used has significant influence on the absorbed energy. Failure mode of tri-tubular conical energy absorber was presented and discussed.

ARTICLE HISTORY
Received : 15th May 2023
Revised : 30th Dec. 2023
Accepted : 19th Jan. 2024
Published : 30th Mar. 2024

KEYWORDS
Tri-tubular cone
Crashworthiness
Energy absorption
Axial crushing
Jute-glass/epoxy

1. INTRODUCTION

Fracture mechanism of metal and composite thin-walled tubular structural components received consideration for many researchers due to wide range of applications of these components in design for crashworthiness of energy absorbing equipment [1]. With the development in the transportation and automotive industry, thin walled light weight structural components are increasingly used as an energy absorbing components [2]. The energy absorption and mode of failure of metal tubes under axial compression is influenced by geometrical parameters and material properties of the component [3]. Tubes of different cross sections such as circular [4], square [5], hexagonal [6] and conical [7] were investigated under axial compression and used as energy absorbers for different applications. Khalid et al. [7] investigated the performance of composite cones made of glass and cotton/ epoxy under axial compression. The authors found that the load increases with increasing the crush distance for the materials used. Composite cones supported higher loads and absorb higher energy with increasing the cone semi-apical angle from 5° to 20° [7]. In recent years, many research work were performed on crushing behavior of bi-tubular components of different cross sections such as triangular [8], circular [9, 10], square [11, 12], and hybrid circular-square and circular-pentagonal bi-tubular components [13]. Haghi et al. [12] performed axial compression on bi-tubular square tubes. The authors concluded that the energy absorption increased with using combined square tubes of parallel and diamond arrangements. Crushworthness analysis on bitubes under axial compression was performed by Vinayagar et al. [14]. Bitubes were of circular outer tube and inner tube of either triangular, square or hexagonal cross-section. The authors found that the bitubes with hexagonal inner tube exhibited higher specific energy absorption than the other bitubular arrangements and single tubes.The bitubes showed significantly higher average crush force and absorb higher energy than the single tubes [14]. Performance of multitubular structures under axial crushing was conducted by Nagarjun et al. [15]. Multitubes of square and circular cross-sections with stiffners supported higher load and absorb more energy than unstiffned multitubes. Both stiffned and unstiffned multitubes recommended as energy absorbing components for vehicles [15]. Behavior of multi-tubular structures of circular, square and triangular cross sections under axial loading was studied by Kumar et al. [16]. The authors found that energy absorbed by the multi-tubular components of circular and square crosssections was higher than the energy absorbed by the bi-tubular components [16]. In order to enhance the crashworthiness performance and energy absorption of bi-tubular energy absorbers and to obtain lighter weight energy absorber, crashworthiness performance of jute-glass/epoxy tri-tubular cones of three cone arrangements TC-1, TC-2, and TC-3, is selected for this investigation. The selected three cone arrangements either of equal or different cone heights. Where, the behavior of tri-tubular cones of the equal or different cone heights under axial compression has not yet been investigated.

***CORRESPONDING AUTHOR | A. A Khalid** | ✉ asad.khalid@utb.edu.bn

The main objectives of the present study are to investigate the crush behavior and absorbed energy of jute, jute-glass and glass/epoxy tri-tubular cone one using three cone height arrangements under axial compression. Also, the study aims to evaluate the crashworthiness and failure mechanism of the axially crushed tri-tubular conical components.

2. MATERIALS AND METHODS

2.1 Finite Element Modelling

Numerical analysis on jute, glass, and hybrid jute-glass/epoxy tri-tubular cones subjected to quasi-static axial compression has been carried out using nonlinear finite element code LS- DYNA [17]. The geometrical configuration of tri-tubular cone arrangements is shown in Figure 1. As shown in Figure 1, three tri-tubular cone arrangements TC-1, TC-2 and TC-3 were selected. TC-1 tri-tubular cone arrangement design is shown in Figure 1(a), where the inner cone is with the highest hight, while the height of the middle and outer cones are less quarter and half of the inner cone height respectively, TC-2 tri-tubular cone arrangement design is shown in Figure 1(b), where the outer cone is with the highest hight. While the height of the middle and inner cones are less quarter and half of the outer cone height respectively. TC-3 tri-tubular cone arrangement design is shown in Figure 1(c), where all the three cones are of the same height. The three design parameters of the tri-tubular cones are designed to investigate the influence of tri-tubular cone arrangement on the crashworthness performances and the absorbed energy. The tri-tubular cone arrangements were selected to investigate the effect of material type and material amount represented by using shorter length cones on the crashworthness performance and energy absorption of the tri-tubular cones. The LS-DYNA software is designed for dynamic analysis. To perform the quasi-static analysis, the mass of the cone and tube materials is scaled up by a factor of 1000. This procedure decreases the time steps required to improve the computation efficiency. To ensure that the static analysis is implemented, the kinetic energy to the internal energy ratio has to be lower than 5% during the compression loading [16–18].

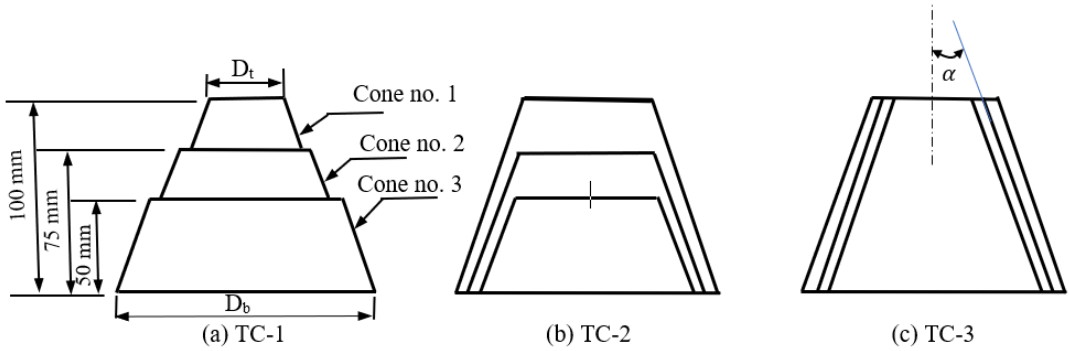

Figure 1. Tri-tubular cone design arrangements

TC-1 represents the three cones with heights of 100 mm, 75 mm and 50 mm respectively starting from the inner cone height. TC-2 represents the three cones with heights of 50 mm,75 mm and 100 mm respectively starting from the inner cone height. While TC-3 represents the three cones with same height of 100 mm. D_t and D_b are cone top and bottom diameters respectively. Cone semi apical angle α is taken as 20°, where this angle can produce optimum failure load and better fracture mechanism to the cones under axial crushing load [7]**.** Design parameters of the tri-tubular cones used in this investigation are shown in Table 1. As shown in the Table 1, the terms TC-1, TC-2 and TC-3 refer to the tri-tubular cone arrangement type.

Table 1. Design parameters of the tri-tubular cones

Properties / Arrangement Type	Cone No.	Top Diameter, D_t (mm)	Bottom Diameter, D_b (mm)	Height, h (mm)	Semi-apical Angle, α (°)
TC-1	1	43.6	116.4	100	20
	2	75.0	129.6	75	
	3	106.4	142.8	50	
TC-2	1	80.0	116.4	50	
	2	75.0	129.6	75	
	3	70.0	142.8	100	
TC-3	1	43.6	116.4	100	
	2	56.8	129.6		
	3	70.0	142.8		

2.2 Element Type and Material Model

Belytschko-Tsay quadrilateral shell elements were used to model the tri-tubular cone component, top and bottom plates [17]. MAT_54/55_ ENHANCED_ COMPOSITE_ DAMAGE material model is used to model the Tri-tubular composite cones. This material model permits the option of using either the Tsai-Wu failure criterion or the Chang-Chang failure criterion for lamina [17]. Material properties are shown in Table 2 [21]. MAT_020_RIGID material model is used to represent the top and bottom steel plates. This material model is assigned for rigid parts in LS DYNA. Rigid plates density, elastic modulus and Poisson's ratio are 7830 kg/m^3, 207× 10^9 N/m^2 and 0.3 respectively.

Table 2. Material properties of glass and jute/epoxy [21]

Parameter(s)	Description	Glass/Epoxy [±45°]	Jute/Epoxy [±45°]
ρ	Density (kg/mm^3)	2.1×10^{-6}	1.6×10^{-6}
E_{11}	Young's Modulus in longitudinal direction (MPa)	52250	17680
E_{22}	Young's Modulus in transverse direction (MPa)	52250	17680
G_{12}	In-plane shear modulus (MPa)	3080	3002
G_{23}	Out of plane shear modulus (MPa)	4200	2860
υ_{23}	Minor Poisson's ratio	0.35	0.29
X_t	Longitudinal tensile strength (MPa)	750	560
X_c	Longitudinal compressive strength (MPa)	430	380
Y_t	Transverse tensile strength (MPa)	38	29
Y_c	Transverse compressive strength (MPa)	136	98
S_c	In plane shear strength (MPa)	67	45

2.3 Boundary Constraints

The tri-tubular model consists of three cones placed between two rigid plates; all modelled by shell elements with thickness of 3 mm. Figure 2 shows the finite element model. The upper rigid plate permits vertical direction movement, while the lower rigid plate is fully prevented from motion. BOUNDARY_PRESCRIBED_MOTION_RIGID command is used to give motion to the upper rigid plate downward. CONTACT_AUTOMATIC_SURFACE_TO_SURFACE algorithm is used to model the interaction between the tri-tubular cone components and rigid plates. Interpenetration between cone walls during progressive folding is prevented throughout releasing the penetrating nodes using CONTACT_AUTOMATIC_SINGLE_SURFACE algorithm. In addition, this type of contact is used to check self interaction of the tri-tubular elements that are in contact during axial crushing process.

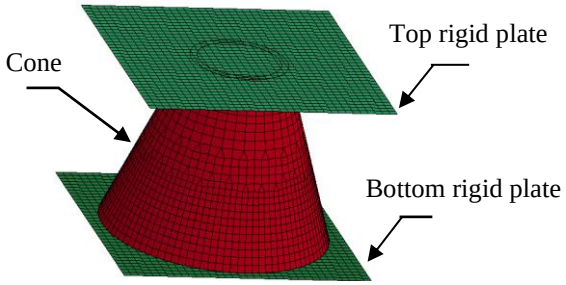

Figure 2. FEA model of tri-tubular cone and the rigid plates

3. RESULTS AND DISCUSSION

3.1 Model Validation

Results of the finite element analysis (FEA) using LS-DYNA software were validated with the experimental results obtained by Kathiresan et al. [22] for single aluminum cone under axial compression loading. Cone length, thickness, and semi apical angle were 95 mm, 0.87 mm and 16°, respectively. Density, Young's modulus and poisson's ratio of aluminium material were; ρ = 2710 kg/m^3, E = 70 Gpa and v = 0.3, respectively. MAT_024_PIECEWISE-_LINEAR_PLASTICITY material model is used to model the aluminum material. This material model is used to represent the deformation of the materials in crush analysis. By using 'MAT_024 piecewise linear plasticity' keyword in LS-DYNA, an isotropic elastic–plastic material model is implemented to represent the aluminum material. Failure mode of the aluminum cone under axial compression obtained by the FEA and failure mode of experimentally tested cone by Kathiresan et al. [22] are shown in Figure 3(a) and 3(b). Progressive failure mode is obtained by the FEA similar to that obtained by the experimental results [22]. Validation of the results is shown in Table 3. Finite element results show a good agreement with the experimental results obtained by Kathiresan et al. [22].

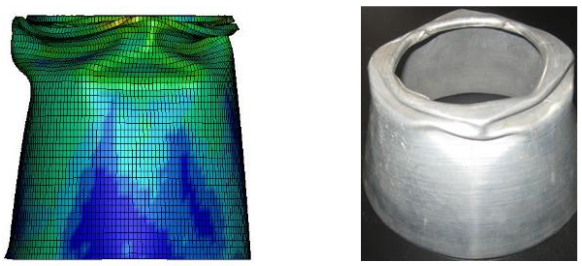

(a) (b)

Figure 3. Failure mode of single cone under axial compression obtained by: (a) FEA analysis and (b) Experimental performed by [22]

Table 3. Validation of the finite element results with experimental results

Material Property	Exp.	FEA	Percentage Difference (%)
Initial Failure Load (kN)	10.30	11.00	6.79
Mean Load (kN)	10.00	10.52	5.20
Maximum Load (kN)	11.70	12.24	4.61
Total Absorbed Energy (J)	200	219	9.50

In addition, finite element analysis results were validated with the simulation results using ABAQUS software obtained by Kumar et al. [16] of bi-tubes under axial loading. Figure 4 shows the load-displacement of bi-tubes under axial loading. Results of load-displacement show a good agreement with the numerical analysis results obtained by Kumar et al. [16]. MAT_024_PIECEWISE_LINEAR_PLASTICITY material model is used to model the Aluminum material. Aluminum density, modulus of elasticity and Poisson's ratio are 2700 kg/m^3, 68×10^9 N/m^2, and 0.3, respectively.

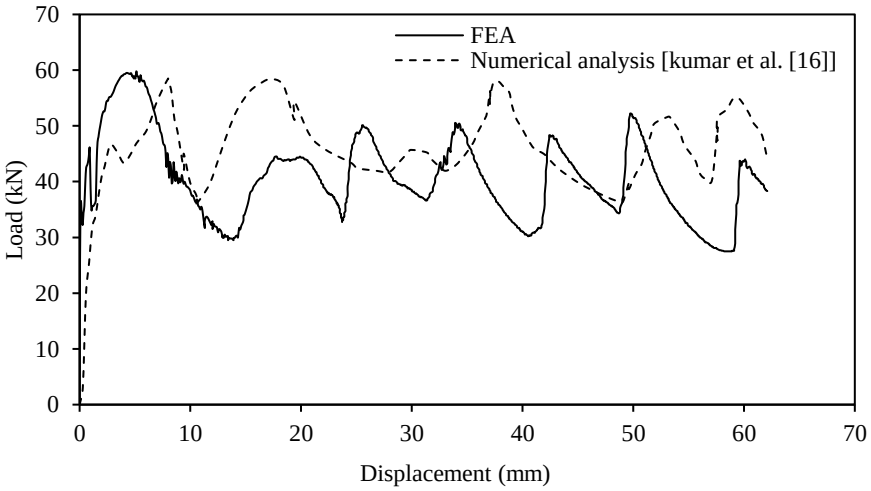

Figure 4. Load-Displacement relation for FEA and result obtained by Kumar et al. [16] of bi-tubes under axial compression

Failure mode of the bi-tubes under axial compression obtained by the FEA analysis and simulation performed by Kumar et al. [16] is shown in Figure 5(a) and (b). Bi-tubular structure of circle and square cross-section tubes was subjected to axial compression. Progressive failure mode obtained by the FEA is similar to that obtained by the numerical analyses [16]. Validation of the results is shown in Table 4.

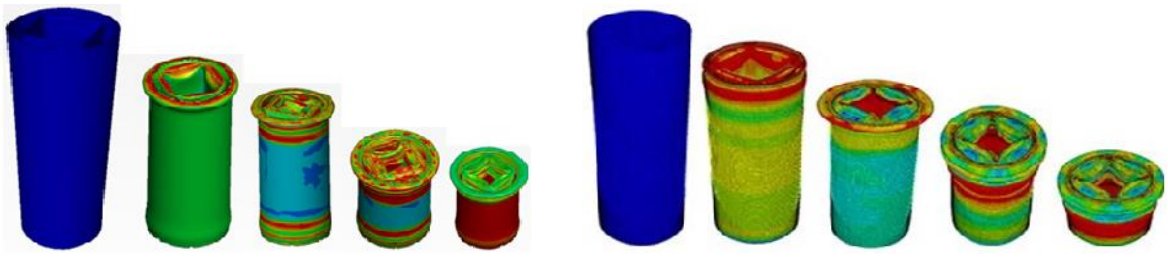

(a) (b)

Figure 5. Failure mode of bi-tubes under axial compression obtained by: (a) FEA analysis and (b) Numerical analysis performed by [16]

Table 4. Validation of the results with numerical analysis

Parameter	Numerical Analysis by Kumar et al. [16]	FEA	Percentage Difference (%)
F_i (kN)	46.71	45.97	1.60
F_m (kN)	45.58	43.75	4.18
F_{max} (kN)	58.43	59.51	1.84

3.2 Crushing Characteristics

Load-displacement results for the jute, glass and jute-glass/epoxy tri-tubular cones are shown in Figure 6. Each cone consists of two layers. The term TC represents tri-tubular cone. The numbers 1, 2 and 3 attached to TC represent the arrangement type of tri-tubular cone as indicated in Figure 6. The term 'a' represents two layers. The load increased with crush distance after the initial peak load and fluctuates until fracturing the cone. For the tri-tubular cone model TC-1a (Figure 6(a)) , after the initial peak load, the load increased with fluctuations until reach the maximum compaction. There are another two peak loads during the crushing process that represent the initial peak loads for cones 2 and 3 respectively. The three main peak loads can be noticed on Figure 6(a). For the Tri-tubular cone model TC-2a (Figure 6(b)), after the initial peak load, the other two peak loads are higher than the case TC-1a. This is attributed to the increase in cone diameters for the case TC-2a with the crush distance compared to the case TC-1a, where the load applied first on the outer cone (cone 3) with larger diameter for the case of TC-2a. While the load applied on the inner cone (cone 1) with smaller diameter for the case of TC-1a. Using hybrid material of jute-glass/epoxy for tri-tubular cones under axial compression increased the load carrying capacity of jute/ epoxy significantly. Tri-tubular cones in case TC-3a (Figure 6(c)) withstand higher load than the other two cases where the three cones are with the same height and the load was applied on the three cones at the same time.

In general, for tri-tubular cones under compression, the load increased with crush distance, where the cone diameter increased with the crush distance until complete fracture. The tri-tubular cone type TC-3a withstand load higher 7.09 % and 14.96 % than the tri-tubular cone types TC-2a and TC-1a respectively for glass/epoxy. For the case of hybrid jute-glass/epoxy tri-tubular cone type the maximum load supported by TC-3a was found higher 5.36 % and 9.48 % than TC-2a and TC-1a, respectively. While the percentage difference was 10.85 % and 16.44 % for jute/epoxy.

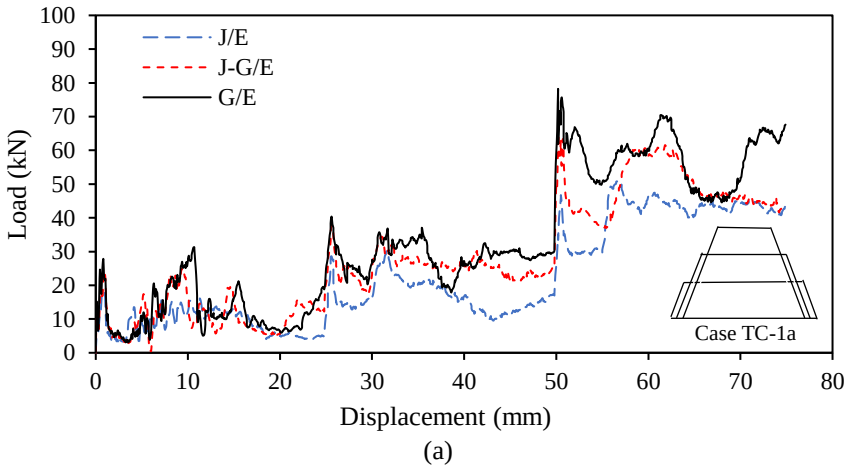

(a)

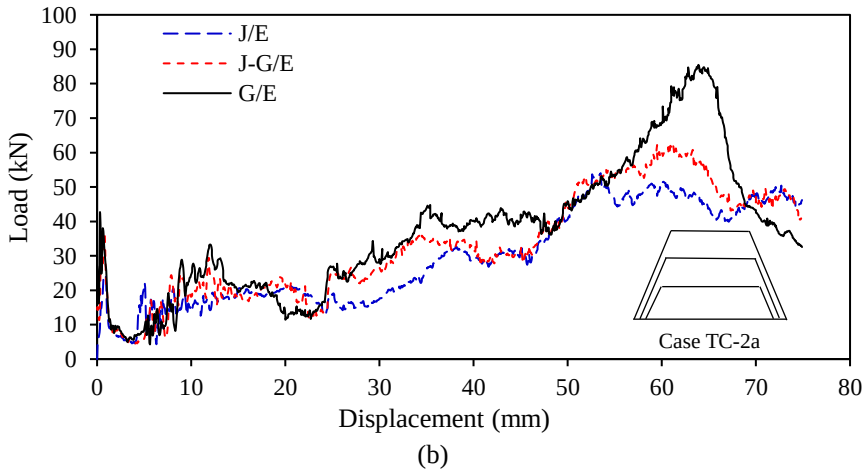

(b)

Figure 6. Load- Displacement relation of tri-tubular cones under axial compression for three different model arrangements: (a) TC-1a (b) TC-2a

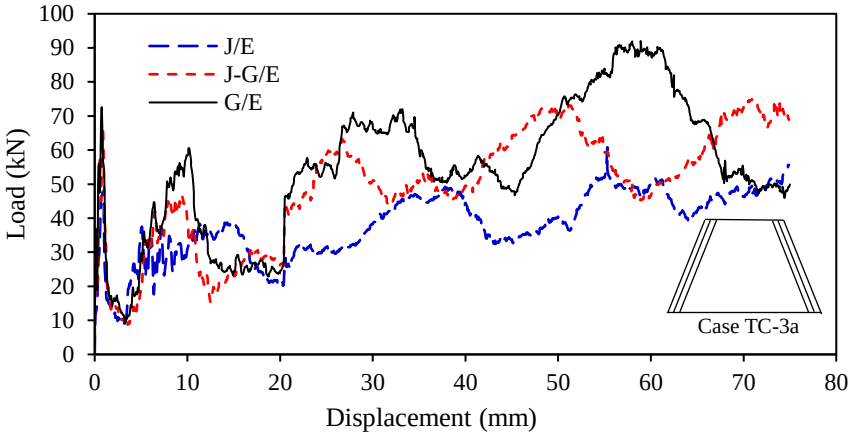

Figure 6. (cont.) (c) TC-3a

Figures 7 and 8 show the effect of tri-tubular cone arrangement on the initial failure load and maximum load. A significant increase in the initial failure load and maximum load is obtained with increasing number of layers from 2 to 4 layers. The terms 'a' and 'b' represent 2 and 4 layers, respectively. Glass/epoxy tri-tubular cones withstand load higher significantly than jute-glass/epoxy followed by jute/epoxy tri-tubular cones. It can be noticed from Figures 7 and 8 that the cone arrangement has influence on the initial and maximum load.

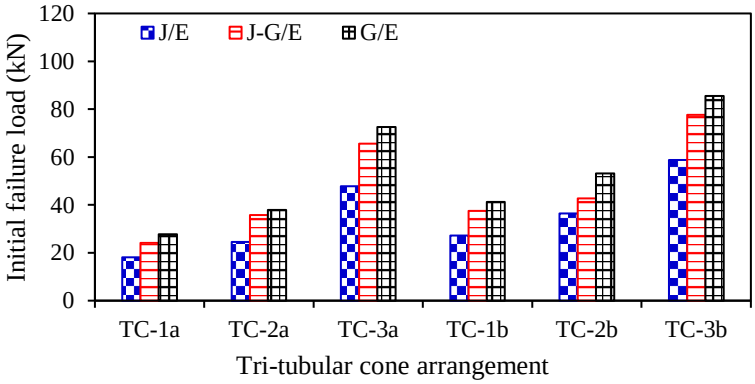

Figure 7. Initial peak compression load of tri-tubular cones

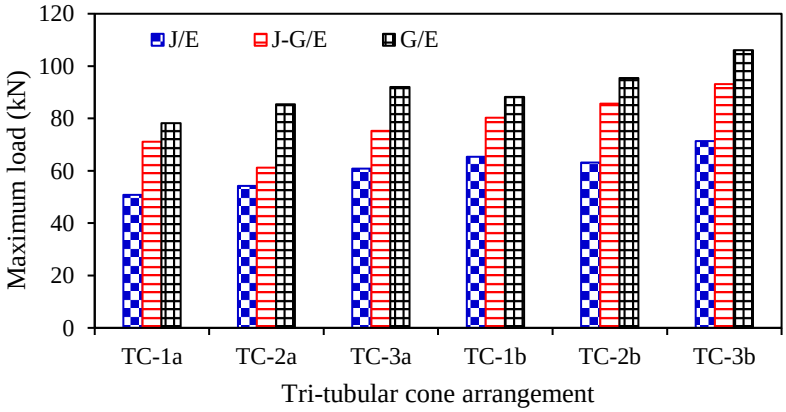

Figure 8. Maximum compression load of tri-tubular cones

3.3 Mean Crush Load and Crush Force Efficiency

The mean crush load, F_{mean} and the crush force efficiency (*CFE*) can be determined as in Eqs. (1) and (2), respectively [6].

$$F_{mean} = \frac{\int_0^{\delta_{max}} F d\delta}{\delta_{max}} \quad (1)$$

$$CFE = \frac{F_{mean}}{F_{max}} \quad (2)$$

Figure 9(a) and (b) shows the influence of the tri-tubular cone arrangement on the mean crush load and crush force efficiency. The mean crush load and crush force efficiency of two layers glass/epoxy tri-tubular cones were found higher than that obtained by jute-glass/epoxy followed by jute/epoxy. The mean crush load of jute-glass epoxy tri-tubular cone arrangement TC-3a was found higher 12.87 % and 21.57 % than that obtained by tri-tubular cone arrangements TC-2a and TC-1a, respectively. The crush force efficiency of two layers of glass/epoxy tri-tubular cones type TC-3a was found higher 7.21 % and 13.04 % than that obtained by jute-glass and jute/epoxy respectively. The percentage of difference in the crush force efficiency for the tri-tubular cones type TC-2a was 11.34 % and 13.79 %, respectively. While the the percentage difference for the the tri-tubular cones type TC-1a was 14.86 % and 23.75 %. In general, the increase in number of layers from two to 4 layers, increased the mean crush load and crush force efficiency significantly.

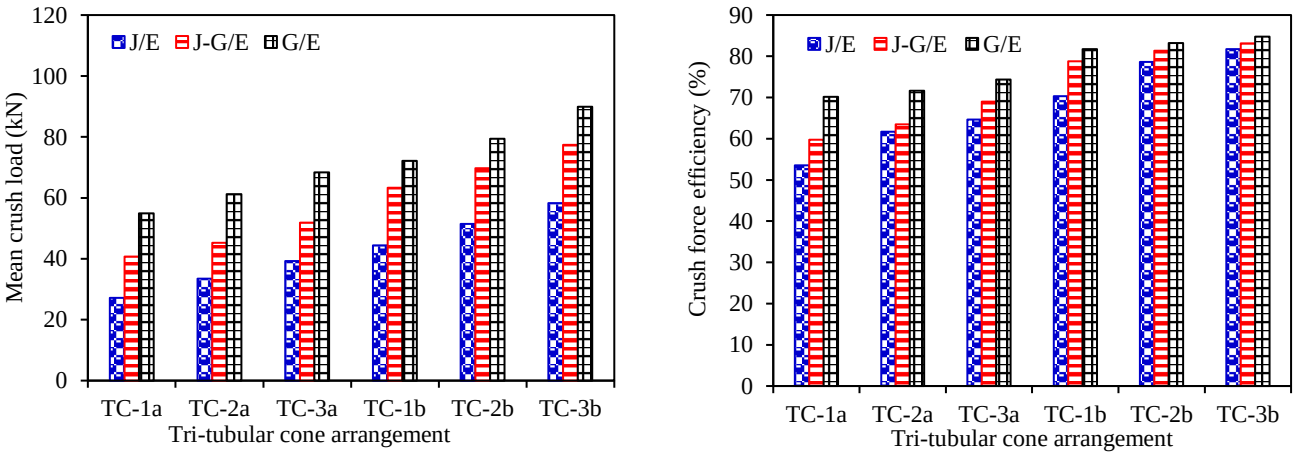

Figure 9. Effect of tri-tubular cone arrangement on: (a) Mean crush load and (b) Crush force efficiency

3.4 Specific Energy Absorption

In this section, the specific energy absorption (*SEA*) is calculated for bi-tubular cone specimens. The *SEA* is an important factor to be considered for the crashworthiness analysis of the energy absorbing structures. The specific energy is the total energy absorbed, E_A per unit mass, m of the energy absorbing component [6] as in Eq. (3):

$$SEA = \frac{E_A}{m} \tag{3}$$

$$E_A = \int_0^{\delta_{max}} F(d\delta) \tag{4}$$

The total energy absorbed by the cones under axial crushing is described as the area under the load-displacement graph. F is the crushing force and δ is the displacement in axial direction. Specific energy absorption for jute, jute-glass, and glass/epoxy tri-tubular cones is shown in Figure 10, where 'a' and 'b' in the x-axis represent two and four layers, respectively. While TC-1, TC-2 and TC-3 represent the three cone model arrangements used in this research.

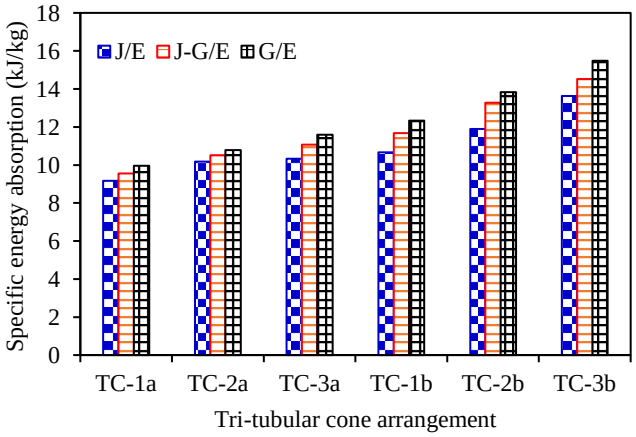

Figure 10. Specific energy absorption of all tri-tubular specimens under axial compression

The two layers of glass/epoxy tri-tubular cones type TC-3a absorbed energy higher 4.65 % and 10.94 % than that obtained by jute-glass and jute/epoxy tri-tubular cones. The percentage difference of tri-tubular cones type TC-2a was 2.5 % and 5.5%. While for the tri-tubular cones type TC-1a, the percentage difference obtained was 4.01% and 7.93% respectively. As shown in Figure 10, the increase in number of layers from 2 to 4, increased the specific energy absorption. Comparison between the absorbed energy of tri-tubular cones and the absorbed energy of three single cones under compression is shown in Figure 11. As shown, the absorbed energy of tri-tubular cons under compression slightly higher in a percentage of 3 % to 8.5 % than the combined energy obtained from three single cones. Results of the tested tri-tubular cones under axial compression are shown in Table 5.

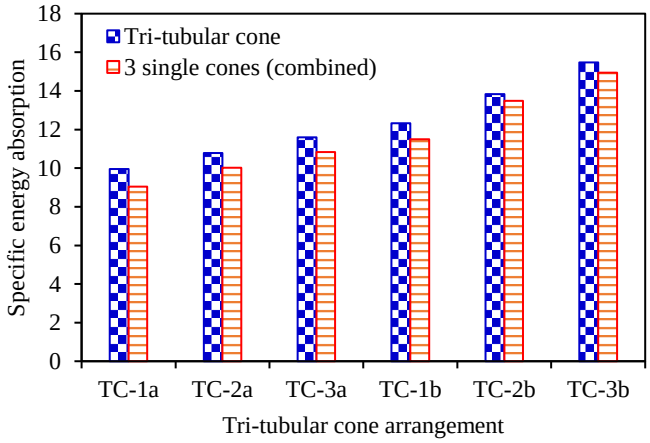

Figure 11. Comparison of specific energy absorption of glass/epoxy tri-tubular cones and combined 3 single cones

Table 5. Results of tri-tubular cones under axial compression

Material	Specimen	mass	F_i	F_{max}	E_t	*SEA*	F_{mean}	*CFE*
		(Kg)	(kN)	(kN)	(kJ)	(kJ/Kg)	(kN)	(%)
J/E	TC-1a	0.216	18.1	50.80	1.98	9.17	27.18	53.51
	TC-2a	0.218	24.5	54.20	2.22	10.18	33.45	61.72
	TC-3a	0.300	47.7	60.80	3.1	10.33	39.30	64.64
	TC-1b	0.408	27.3	63.20	4.35	10.66	44.45	70.34
	TC-2b	0.433	36.5	65.40	5.15	11.89	51.43	78.64
	TC-3b	0.519	58.7	71.30	7.07	13.62	58.30	81.77
J-G/E	TC-1a	0.225	24.1	68.10	2.15	9.56	40.70	59.75
	TC-2a	0.237	35.7	71.20	2.49	10.51	45.22	63.48
	TC-3a	0.310	65.6	75.24	3.43	11.06	51.90	68.98
	TC-1b	0.471	37.5	80.34	5.5	11.68	63.31	78.79
	TC-2b	0.501	42.7	85.70	6.65	13.27	69.70	81.33
	TC-3b	0.601	77.6	93.11	8.73	14.53	77.40	83.13
G/E	TC-1a	0.240	27.7	78.23	2.39	9.96	54.90	70.18
	TC-2a	0.245	37.9	85.47	2.64	10.78	61.21	71.60
	TC-3a	0.300	72.6	92.00	3.48	11.60	68.40	74.34
	TC-1b	0.481	41.2	88.23	5.93	12.33	72.13	81.72
	TC-2b	0.501	53.1	95.47	6.93	13.83	79.40	83.17
	TC-3b	0.581	85.5	106.1	8.99	15.47	89.90	84.73

Results obtained show that the absorbed energy and crashworthness performance of the three tri-tubular cone arrangements enhanced when hybrid jute-glass/epoxy material is used in comparison with the jute/epoxy material. Hybridize jute natural fiber with glass synthetic fiber will add advantages and resulted in forming an energy absorber that have lighter weight and lower cost, less toxic and environmentally friendly material, have a moderate energy absorbtion between jute/epoxy and glass/epoxy. In addition, the results of the current research show that the crashworthness performance of tri-tubular cone arrangements TC-1 and TC-2 energy absorbers of three different cone heights produced energy absorber of lighter weight with acceptable level of performance compared to that obtained by TC-3 tri-tubular cone arrangement that conststs of thee cones with the same height. In general, when adding energy absorption device to an automotive and structural components that are exposed to loads, the tri-tubular cone energy absorber withstands high

loads, exhibits high energy absorption and crush progressively, which enhance the performance of the energy absorber and provide additional safety to protect human lifes when the crushing occurs.

3.5 Failure Mode

Failure mode of the jute, jute-glass and glass/epoxy tubes represented by von-Mises stress contours is shown in Figure 12. For each material used, failure modes of three tri-tubular cone design arrangements TC-1a, TC-2a and TC-3a are introduced. From the figure, it can be noticed that the energy was absorbed by fiber/epoxy composite cones and increased with the progress in the crush distance. The distinctive fracture modes are fiber breaking, matrix cracking, delamination, fragmentation and splaying. Among all the tested tube configurations, it is found that the tri-tubular cones crushed from the upper section where the inner cone absorbed less amount of energy compared to the outer cone.

The first contact between the top rigid plate and the first cone of specimen TC-1a results in progressive crushing mode without any debris splitting. Then fiber delamination occurs, and due to the increase in cone cross section area the energy increases and load fluctuates due to fiber break and matrix cracking with the progress in crushing. The absorbed energy increases when the crush distance reaches the top surface of the second cone followed by the third cone. Progressive failure mode is obsered on the first, second and third cone. This creates a repeating trend on the load-displacement relation but with higher loads for the second and third cones as the resistance to the load increased due to the increase in the cross section area of the cone.

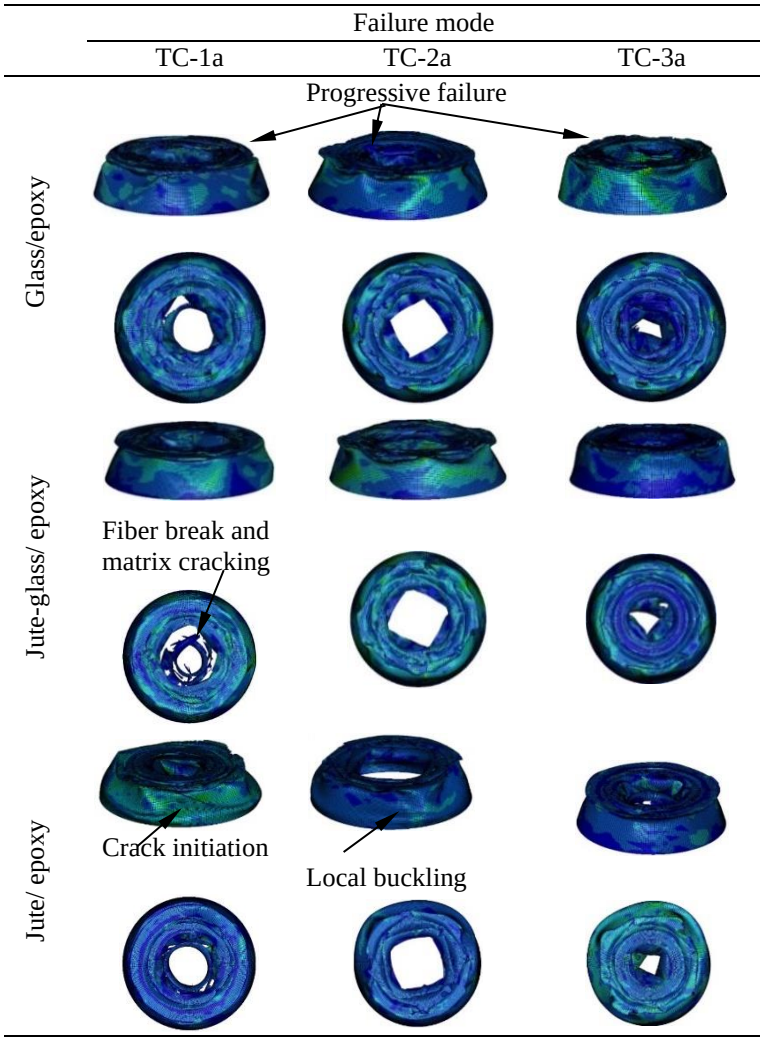

Figure 12. Failure mode of the axially crushed tri-tubular cones

Specimen TC-2a with 2 layers of glass/epoxy shows a progressive failure mode similar to that of TC-1a with a different load level with the progress in the crushing distance. The absorbed energy of this cone is higher than that in case TC-1a due to increase in the cone cross section area where the outer cone progressively crushed first. The crushing load levels increased when the crush distance reach to middle cone followed by the inner cone. In TC-2a, the outer cone folds toward the inner side of the cone as the crushing distance increases and this creates a stable load-displacement curve. For tri-tubular cone arrangement TC-3a all cones are crushed at the same time where the three cones are with the same height. Second type of failure mode noticed on the tri-tubular cones is buckling mode. This mode can be observed by the formation of polygonal shape from the top view. Fiber and matrix cracking also observed. In general, the three cones of the tritubular cone arrangement type TC-3, crush progressively at the same time time. For the TC-1 and TC-2 tritubular

cone arrangements, the crushing process start on the highest cone of height 100 mm followed be the cone of 75 mm height and then the cone of 50 mm height. the decrease in cone length decreases the amount of material used for the energy absorber.

4. CONCLUSIONS

In this research, finite element analysis has been carried out to investigate the crashworthiness and failure mechanism of tri-tubular cones under axial compression. Three types of tritubular cone arrangements TC-1, TC-2 and TC-3 were investigated. The main conclusions that could be drawn from this investigation are:

i) Tri-tubular cone arrangement TC-3 withstand higher axial compression loads than the TC-2 and TC-1 tri-tubular cone types respectively. For two layers glass/epoxy tri-tubular cones, the tri-tubular cone type TC-3a supported load higher 7.09 % and 14.96 % than the tri-tubular cone types of TC-2a and TC-1a respectively.

ii) Energy absorbed by two layers of glass/epoxy tri-tubular cones type TC-3 was found higher 4.65 % and 10.94 % than jute-glass and jute/epoxy tri-tubular cones respectively.

iii) Using hybrid jute-glass/epoxy material gives a moderate result between the results obtained by using glass/epoxy and jute/epoxy. In addition, hybridize jute/epoxy with glass/epoxy resulted in less toxic material to the environment.

iv) The tri-tubular cone arrangement increased total absorbed energy and specific energy absorption compared to the absorbed energy obtained from combined single cones. Furthermore, the tri-tubular cone arrangement gives better crashworthiness response than that obtained from three single cones.

v) Progressive crushing failure and local buckling failure modes are observed on the tested tri-tubular cones. In addition, fiber-breaking, matrix cracking, delamination, fragmentation, and splaying modes of failure were observed.

vi) The tri-tubular cone arrangements TC-1 and TC-2 of three different cone heights, reduced the amount of material represented by cone heights compared with the tri-tubular cone arrangement TC-3 that consists of three cones of equal height, resulted in lighter weight tri-tubular energy absorber.

vii) For the TC-3 tri-tubular cone arrangement, all cones progressively crushed at the same time. While for the TC-1 and TC-2, the axial crushing process started on the highest cone of 100 mm length and progressively crushed first, the second cone of 75 mm length start to crush, followed by the third cone of 50 mm length.

5. ACKNOWLEDGMENTS

The authors would like to acknowledge the Faculty of Engineering at Universiti Teknologi Brunei for providing the necessary equipment and software to conduct the present research.

6. REFERENCES

[1] N. K. Gupta, H. Abbas, “Lateral collapse of composite cylindrical tubes between flat platens,” *International. Journal of Impact Engineering.*, vol. 24, no. 4, pp. 329–346, 2000.

[2] A. P. Kumar, “Experimental analysis on the axial crushing and energy absorption characteristics of novel hybrid aluminum/composite-capped cylindrical tubular structures,” *Proceedings of the Institution of Mechanical Engineers, Mechanical Engineering Part L: Journal of Materials: Design and Applications*, vol. 233, no. 11, pp. 2234–2252, 2019.

[3] D. Hull, “A unified approach to progressive crushing of fibre-reinforced composite tubes,” *Composites Science and Technology*, vol. 40, no. 4, pp. 377–421, 1991.

[4] X. Liu, B. Belkassem, A. Jonet, D. Lecompte, D. Van Hemelrijck, R. Pintelon, L. Pyl, “Experimental investigation of energy absorption behaviour of circular carbon/epoxy composite tubes under quasi-static and dynamic crush loading,” *Composite Structures*, vol. 227, p. 111266, 2019.

[5] S. A. Oshkovr, R. A. Eshkoor, S. T. Taher, A. K. Ariffin, C. H. Azhari, “Crashworthiness characteristics investigation of silk/epoxy composite square tubes,” *Composite Structures*, vol. 94, no. 8, pp. 2337–2342, 2012.

[6] M. A. Guler, M. E. Cerit, B. Bayram, B. Gerçeker, E. Karakaya, “The effect of geometrical parameters on the energy absorption characteristics of thin-walled structures under axial impact loading,” *International Journal of Crashworthiness*, vol. 15, no. 4, pp. 377–390, 2010.

[7] A. A. Khalid, B. B. Sahari, Y. A. Khalid, “Performance of composite cones under axial compression loading,” *Composites Science and Technolgy*, vol. 62, no. 1, pp. 17–27, 2002.

[8] A. Praveen Kumar, M. Yadi Reddy, M. Shunmugasundaram, “Energy absorption analysis of novel double section triangular tubes subjected to axial impact loading,” *Materials Today: Proceedings*, vol. 47, pp. 5942–5945, 2021.

[9] K. D. Karantza, I. G. Papantoniou, P. K. Kostazos, D. E. Manolakos, "Crashworthiness behavior of thin-walled bimaterial tubes under axial collapse," *Materials Today: Proceedings*, vol. 93, pp. 575–582, 2023.

[10] A. Praveen Kumar, D. Nageswara Rao, "Crushing characteristics of double circular composite tube structures subjected to axial impact loading," *Materials Today: Proceedings*, vol. 47, pp. 5923–5927, 2021.

[11] A. P. Kumar, C. Pradeep, S. Sai Rahul Gupta, G. Vamshi Krishna, G. Harshavardhan, "Impact loading behavior of woven glass fabric polymer composite bi-tubular square sections," *Materials Today: Proceedings*, vol. 47, pp. 6291–6295, 2021.

[12] M. Haghi Kashani, H. Shahsavari Alavijeh, H. Akbarshahi, M. Shakeri, "Bitubular square tubes with different arrangements under quasi-static axial compression loading," *Materials and Design*, vol. 51, pp. 1095–1103, 2013.

[13] A. P. Kumar, D. Sravani, "Experimental assessment of axial deformation behaviour of aluminium-kevlar composite hybrid bitubular structures," *Materials Today: Proceedings*, vol. 47, pp. 5955–5958, 2021.

[14] K. Vinayagar, A. Senthil Kumar, "Crashworthiness analysis of double section bi-tubular thin-walled structures," *Thin-Walled Structures*, vol. 112, pp. 184–193, 2017.

[15] J. Nagarjun, A. Praveen Kumar, K. Yamini Reddy, L. Ponraj Sankar, "Dynamic crushing and energy absorption performance of newly designed multitubular structures," *Materials Today: Proceedings*, vol. 27, no. 2, pp. 1928–1933, 2020.

[16] A. P. Kumar, M. Shunmugasundaram, S. Sivasankar, L. P. Sankar, "Numerical analysis on the axial deformation and energy absorption behaviour of tri-tubular structures," *Materials Today: Proceedings*, vol. 27, pp. 866–870, 2020.

[17] LS-DYNA, Keyword User'S Manual, Version 971 / Release 4 Beta, vol. I, 2009.

[18] K. J. Bathe, J. Walczak, O. Guillermin, P. A. Bouzinov, H. Y. Chen, "Advances in crush analysis," *Computers and Structures*, vol. 72, no. 1, pp. 31–47, 1999.

[19] H. El-Hage, P. K. Mallick, N. Zamani, "A numerical study on the quasi-static axial crush characteristics of square aluminum - Composite hybrid tubes," *Composite Structures*, vol. 73, no. 4, pp. 505–514, 2006.

[20] H. Han, F. Taheri, N. Pegg, Y. Lu, "A numerical study on the axial crushing response of hybrid pultruded and ±45° braided tubes," *Composite Structures*, vol. 80, no. 2, pp. 253–264, 2007.

[21] A. A. Khalid, "Behaviour of hybrid jute-glass/epoxy composite tubes subjected to lateral loading," *IOP Conference Materials Science and Engineering*, vol. 100, no. 1, pp. 1-8, 2015.

[22] M. Kathiresan, K. Manisekar, V. Manikandan, "Performance analysis of fibre metal laminated thin conical frusta under axial compression," *Composite Structures*, vol. 94, no. 12, pp. 3510–3519, 2012.